Int J Clin Exp Med 2018;11(3):1570-1586
www.ijcem.com /ISSN:1940-5901/IJCEM0064977

Original Article

Expression level of miR-146b-5p via miRNA sequencing and its potential targets in papillary thyroid cancer

Lin Shi[1,2*], Peng Lin[3*], Dongyue Wen[3], Li Gao[1], Liang Liang[4], Yihuan Luo[4], Yichen Wei[1], Yu He[3], Hong Yang[3], Wei Ma[1]

Departments of [1]Pathology, [3]Medical Ultrasonography, [4]Gastrointestinal Surgery, The First Affiliated Hospital of Guangxi Medical University, Nanning, People's Republic of China; [2]Department of Pathology, The First Affiliated Hospital of Guangxi University of Science and Technology, Liu Zhou, People's Republic of China. [*]Equal contributors.

Received September 5, 2017; Accepted January 4, 2018; Epub March 15, 2018; Published March 30, 2018

Abstract: *Background and objective:* MiR-146b-5p is one of the deregulated miRNAs in papillary thyroid carcinoma (PTC) that promotes the malignant potential of cancer cells. To interpret the clinical significance and underlying molecular mechanism of miR-146b-5p in PTC, a comprehensive analysis combining The Cancer Genome Atlas (TCGA) data and *in silico* investigation was conducted. *Methods:* Expression and clinical data for PTC were obtained from TCGA, and the relationships between miR-146b and clinicopathological parameters as well as the prognosis were later analyzed. Putative target genes of miR-146-5p were acquired by intersecting the differentially expressed genes of GSE76050 with genes predicted by twelve online software programs. Subsequently, Gene Ontology (GO) enrichment, Kyoto Encyclopedia of Genes and Genomes (KEGG) pathway, and PPI network analyses were performed using the chosen target genes to analyze the probable molecular mechanisms of PTC. Finally, several hub genes were validated via GEPIA and The Human Protein Atlas. *Results:* MiR-146b was strongly overexpressed in PTC tissues as evidenced by TCGA data. MiR-146b levels were also significantly associated with the progression of PTC. In total, 6273 and 4228 genes were identified as potential targets from GSE chip data and online prediction, respectively. Ultimately, 994 genes were chosen as the most probable targets from the intersection of the two gene sets. According to the GO enrichment analysis, 'intracellular signaling cascade', 'regulation of programmed cell death', 'positive regulation of cellular biosynthetic process', 'insoluble fraction', 'cell fraction', 'membrane fraction', 'transcription regulator activity' and 'transcription activator activity' were the most significant GO terms for the target genes. In regard to KEGG analysis, the targets were significantly clustered into cancer, apoptosis, and calcium signaling pathways. Two prospective targets, TRAF1 and PML, were both down-regulated at the mRNA and protein level in PTC tissues. *Conclusions:* MiR-146b-5p may play an essential role in the progression of PTC and influence the biological processes of cancer cells by regulating downstream targets involved in multiple signaling pathways.

Keywords: Papillary thyroid carcinoma, miR-146b-5p, the Cancer Genome Atlas, hub genes

Introduction

Papillary thyroid carcinoma (PTC) is the predominant type of thyroid cancer (TC), constituting approximately 80% of all TCs [1, 2]. PTCs have been classified into several subtypes according to the histological and morphological characteristics, among which PTCs frequently present as multifocal intra-thyroid tumors (65% of all cases) [3, 4]. Despite the fact that current treatments for PTC, such as surgical resection and adjuvant radioactive iodine (RAI) therapy, can provide patients with good prognosis, tumor recurrence accompanied by lymph node metastasis still occurs in some patients [5, 6] and an increasing morbidity of PTC has been reported over the last 40 years [7, 8]. Therefore, better targets are needed to improve their survival.

The initiation and development of PTC is a complicated process involving multiple genes and signaling pathways [9-11]. Although great advancements have been made on the detection of aberrantly expressed and mutated genes including EphB4, EphrinB2, EGFR, p53,

BRAF, RAS, PTEN, and TP53 [12], the molecular pathogenesis of PTC is far from fully elucidated. Recent studies have revealed that abnormally expressed microRNAs (miRNAs) are actively involved in PTC [13, 14]. miRNAs are a class of endogenous non-coding RNAs that suppress the expression of downstream targets by binding to the 3'-untranslated regions of mRNAs [15, 16]. Abundant evidence has suggested that miRNAs play pivotal roles in various human cancers by affecting the growth, proliferation, differentiation, apoptosis, and metastasis of cancer cells [17, 18]. The deregulation of miRNAs has also been observed in PTC [13, 19-22]. Among the miRNAs studied to date, miR-146-5p has been a research hot spot. Prior studies indicated that miR-146b-5p contributes to the metastasis, migration and invasion of cancer cells by interacting with different molecular targets in PTC [18, 23-29]. Nevertheless, the molecular mechanism of miR-146-5p in PTC remains unknown. Furthermore, no study has mined miRNA-seq data to explore the clinical role of miR-146a-5p. Thus, we carried out this study to investigate the clinical role of miR-146-5p in PTC by combining miRNA-seq data and bioinformatics methods to identify its target genes.

Material and methods

MiRNA-seq data mining based on TCGA

Since only the data for precursor miRNA was provided by the miRNA-seq from TCGA, the expression level of precursor miR-146b was downloaded and re-calculated (https://gdc-portal.nci.nih.gov/). Differences in miR-146b levels between PTC tissues and their non-cancerous counterparts, as well as between different groups based on clinical parameters were assessed with a Student's t-test. The diagnostic value of miR-146b was examined by using the receiver operating characteristic (ROC). The prognostic value of miR-146b was evaluated by using Kaplan-Meier analysis. All statistical analysis was conducted with SPSS 22.0 and $P<0.05$ was considered significant.

Optimal candidate target genes of miR-146b-5p

Differentially expressed mRNAs targeted by miR-146b-5p were identified by GSE76050 from the Gene Expression Omnibus (GEO) dataset, an expression profiling array. For this analysis, a control sample of untreated BCPAP cells and a sample transfected with miR-146b-5p mimic in PTC cell lines were included in a two-condition experiment. The processed data (normalized by log10 ratio) were transformed into fold changes, and down-regulated mRNAs with changes of less than 0.5-fold were gathered. Additionally, to obtain the predicted target mRNAs of miR-146b-5p, twelve online prediction programs, including miRWalk, Microt4, miRanda, mirbridge, miRDB, miRMap, miRNAMap, Pictar2, PITA, RNA22, RNAhybrid and Targetscan, were employed in this study. Genes that appeared in the results of at least four of the platforms were selected as potential targets of miR-146b-5p. Next, genes overlapping in the lists from both GSE microarray and prediction software were considered as optimal candidate targets of miR-146b-5p in PTC.

PPI network of target genes

To visualize the interactions between the target genes of miR-146b-5p, a Protein-Protein Interaction network was drawn using STRING (http://www.string-db.org/). Genes with the highest degree values were considered to be hub genes.

Functional annotation of miR-146b-5p target genes

To evaluate the function of the selected target genes, we carried out Gene Ontology (GO) enrichment analysis and KEGG pathway annotation in DAVID (http://david.abcc.ncifcrf.gov/). GO terms classified as biological process (BP), cellular component (CC), molecular function (MF) with a modified Fisher Exact *P*-value less than 0.01 and pathways with *p*-values less than 0.05 were considered to be significant. The GO enrichment analysis was visualized by Cytoscape v3.5.0. Protein-protein interaction (PPI) maps were also plotted to illustrate the network of target genes in the three most significant KEGG signaling.

Validation of the hub target genes of miR-146b-5p

To further verify that the predicted hub genes are real targets of miR-146b-5p in PTC, the mRNA level of the selected genes was shown by GEPIA using TCGA data for analysis.

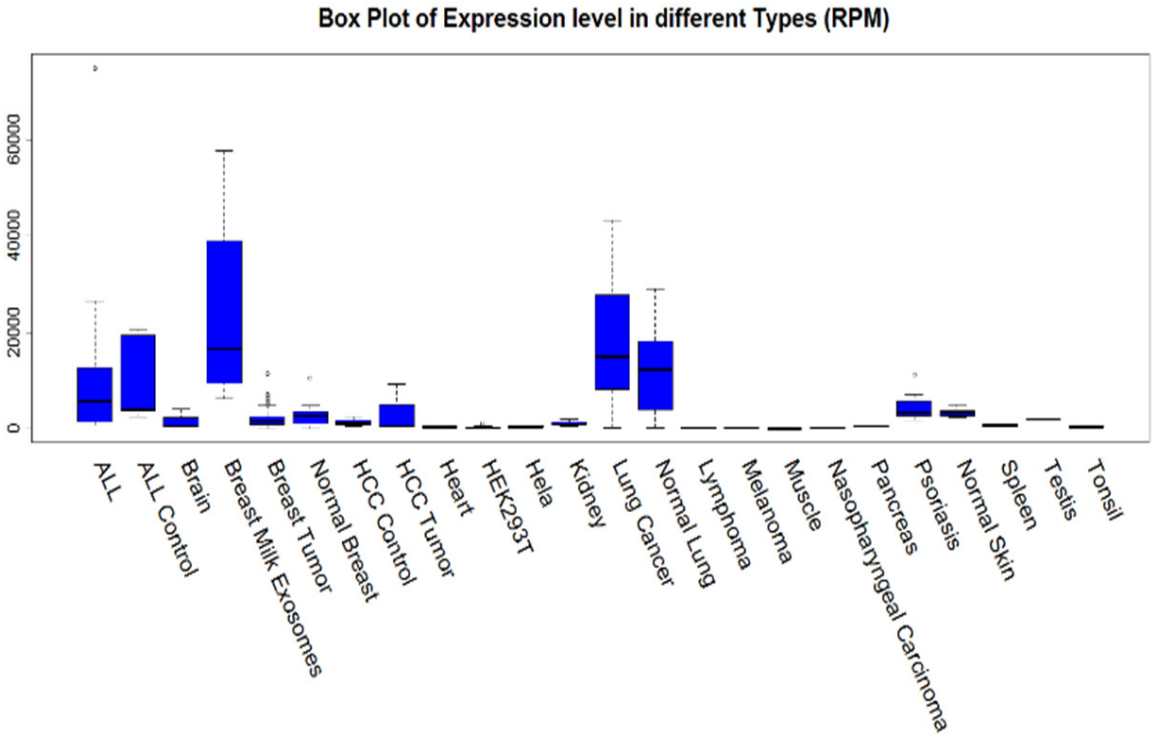

Figure 1. miR-146a-5p expression in different organs and tumors. miR-146a-5p expression data was downloaded from Human MiRNA Expression Database (HMED) (http://bioinfo.life.hust.edu.cn/smallRNA/index.php).

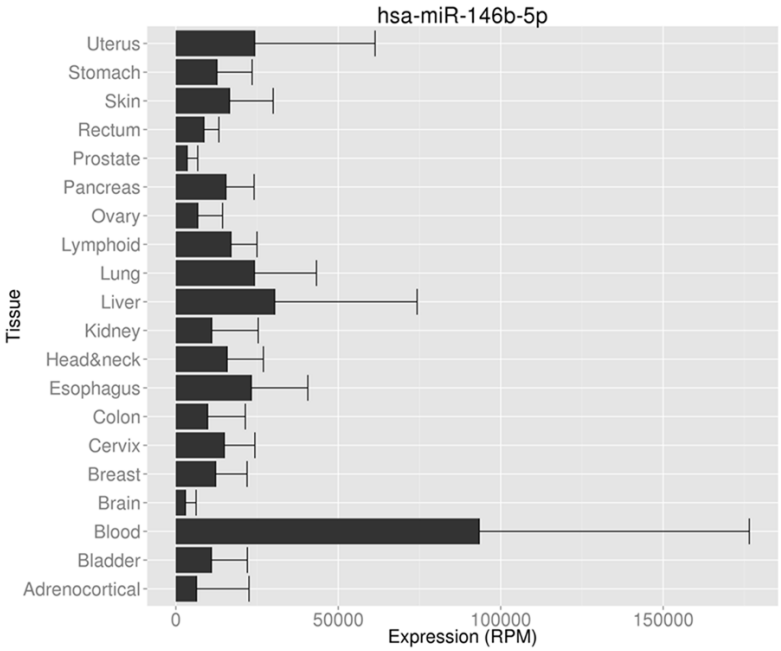

Figure 2. miR-146a-5p expression in different organs. miR-146a-5p expression data were downloaded from YM500v3 (http://driverdb.tms.cmu.edu.tw/ym500v3/knownmir_sample.php).

Simultaneously, protein levels of the genes were displayed via The Human Protein Atlas.

Results

Characteristics of patient cohort and expression of miR-146b in PTC tissues

miR-146b-5p exhibited different expression patterns in different organs and tumors (**Figures 1** and **2**). The PTC cohort in TCGA contained 507 cases of tumor tissues and 59 normal thyroid glands as controls. The level of miR-146b precursor was pronouncedly overexpressed in PTC tissues as evidenced by TCGA data (**Table 1** and **Figure 3A**). More importantly, the AUC of the ROC for miR-146b to diagnose cancer tissues from non-cancerous counterparts was high, with a value of 0.914 (**Figure 3B**). Furthermore, miR-146b levels were significantly higher in cases with lymph node metastasis than without. Patients

Table 1. Relationship between miR-146b expression and clinicopathological parameters in PTC patients

Clinicopathological Features		N	miR-146b relative expression		
			Mean ± SD	t	P
Tissue	Normal thyroid	59	11.116057±1.0881889	-27.043	<0.001
	PTC	507	16.056852±2.5976889		
Gender	Female	368	16.091061±2.5997697	0.595	0.552
	Male	136	15.935675±2.6172809		
Size	<mean	298	16.153317±2.4915347	0.998	0.319
	≥mean	209	15.919308±2.7421695		
Age	<45	228	16.197265±2.3567735	1.180	0.238
	≥45	276	15.926760±2.7880713		
T stage	I-II	312	15.749070±2.7391348	-3.483	0.001
	III-IV	193	16.536118±2.2827869		
N stage	Nx-N0	280	15.229561±2.9487809	-8.973	<0.001
	N1	224	17.073595±1.5825420		
M stage	Mx-M0	494	16.051258±2.6110990	-0.497	0.619
	M1	9	16.485906±1.5780113		
Pathologic stage	I-II	338	15.734840±2.7519345	-4.277	<0.001
	III-IV	167	16.687454±2.1315250		
Focus types	Unifocal	268	16.096057±2.5014009	0.346	0.730
	Multifocal	226	16.015166±2.6948302		
Extrathyroid extension	No	334	15.672182±2.8114920	-6.448	<0.001
	Yes	152	17.012230±1.7226757		
Subtypes	Classical/usual	357	16.654161±2.1341696	a	
	Follicular	103	13.418366±2.8286974		
	Tall cell	37	17.319059±1.1982802		

LSD test: Classical/usual vs. Follicular P<0.001, Classical/usual vs. Tall Cell P=0.086, Follicular vs. Tall Cell P<0.001.

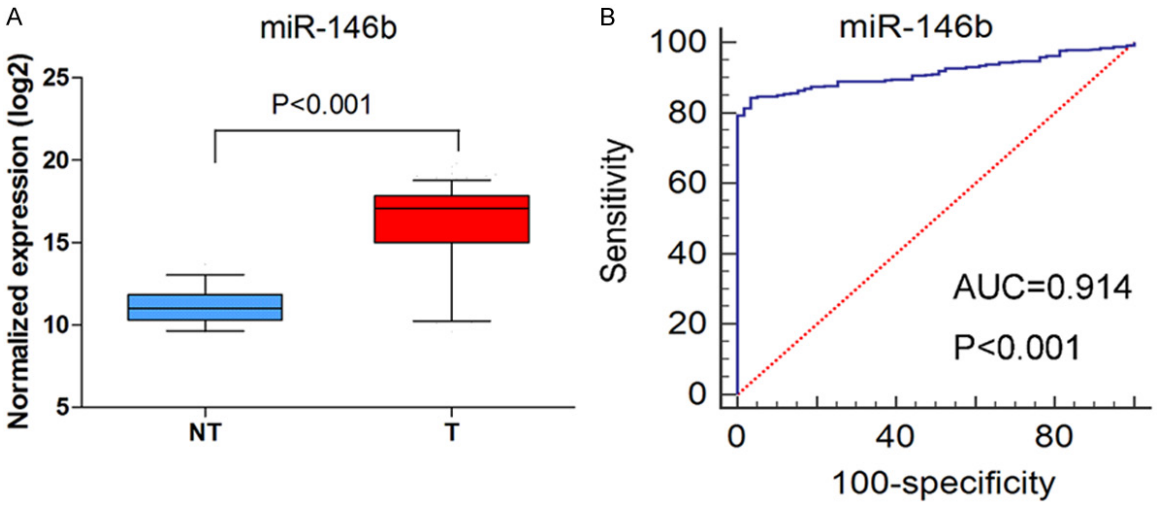

Figure 3. Expression level of precursor miR-146b in thyroid cancer from TCGA. A: NT: non-tumorous tissues; T: tumor. B: ROC curve.

in advanced stages showed higher levels of miR-146b than those in early stages. Moreover, cases with extrathyroid extension also had markedly higher levels of miR-146b compared to those without (**Table 1**). However, miR-146b was not significantly correlated with other clinical parameters, including prognosis (**Table 1** and **Figure 4**).

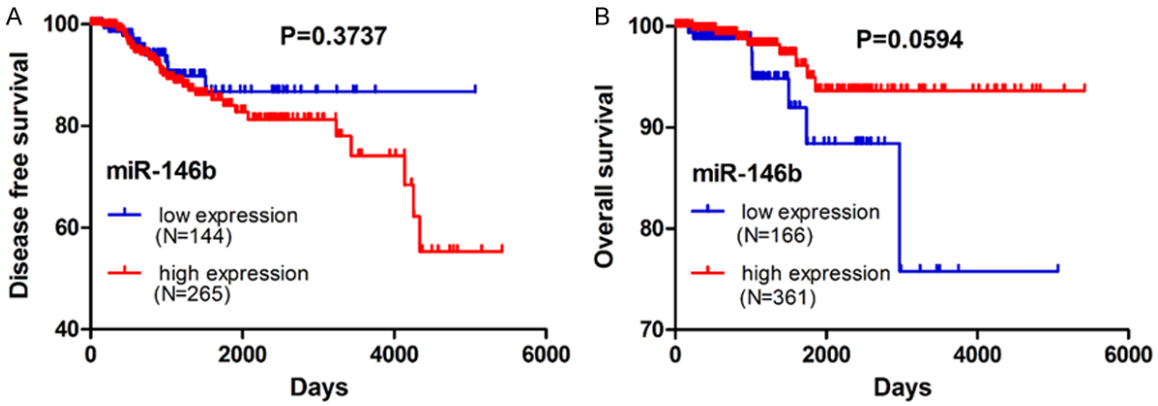

Figure 4. Prognostic value of miR-146b in thyroid cancer from TCGA. A: Disease-free survival; B: Overall survival.

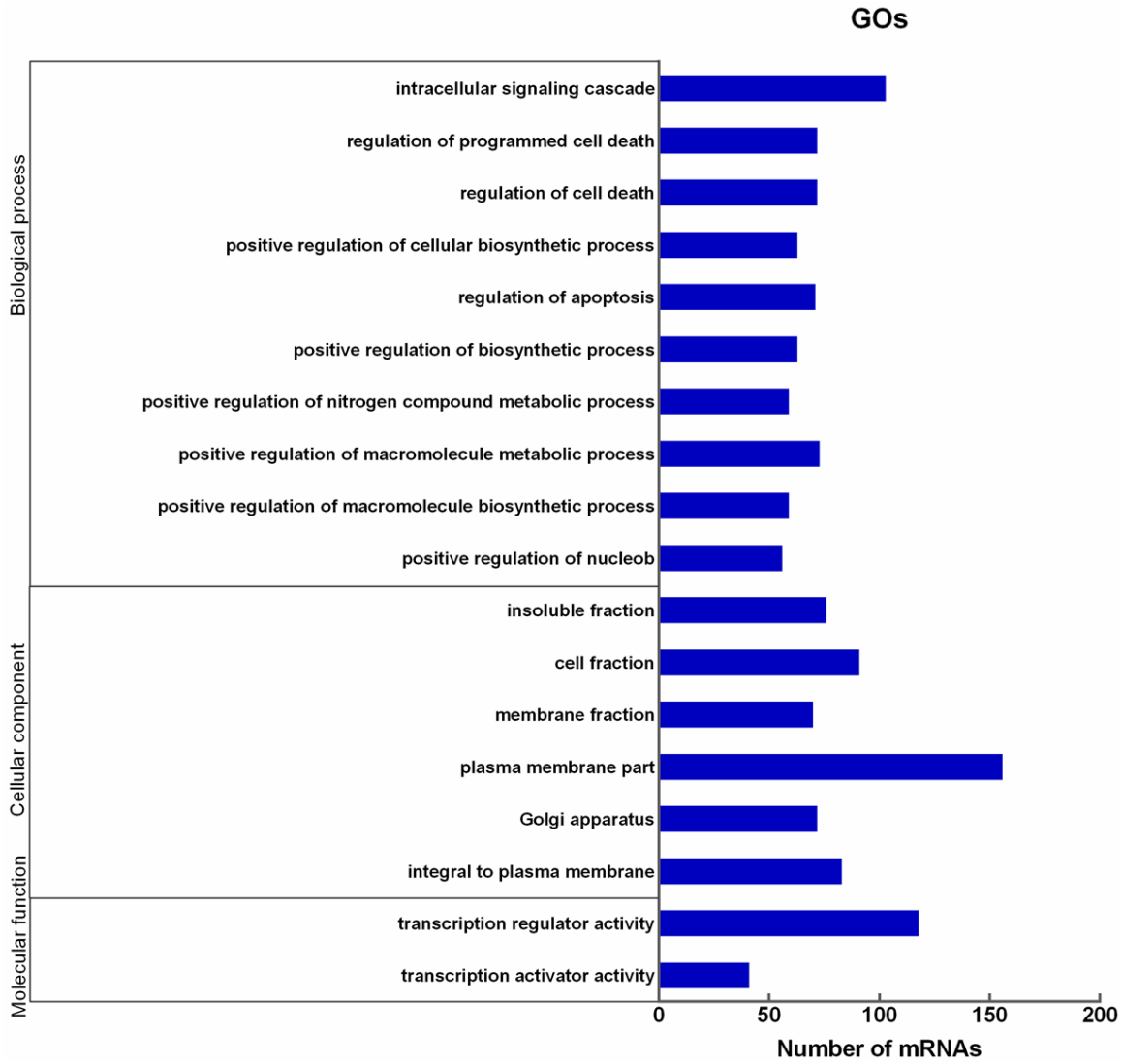

Figure 5. Functional annotation of DAVID GO terms enriched by the potential target mRNAs of miR-146b-5p. The ten most significant GO terms for Biological process (BP) and all significant GO terms for Cellular component (CC) and Molecular function (MF) are displayed.

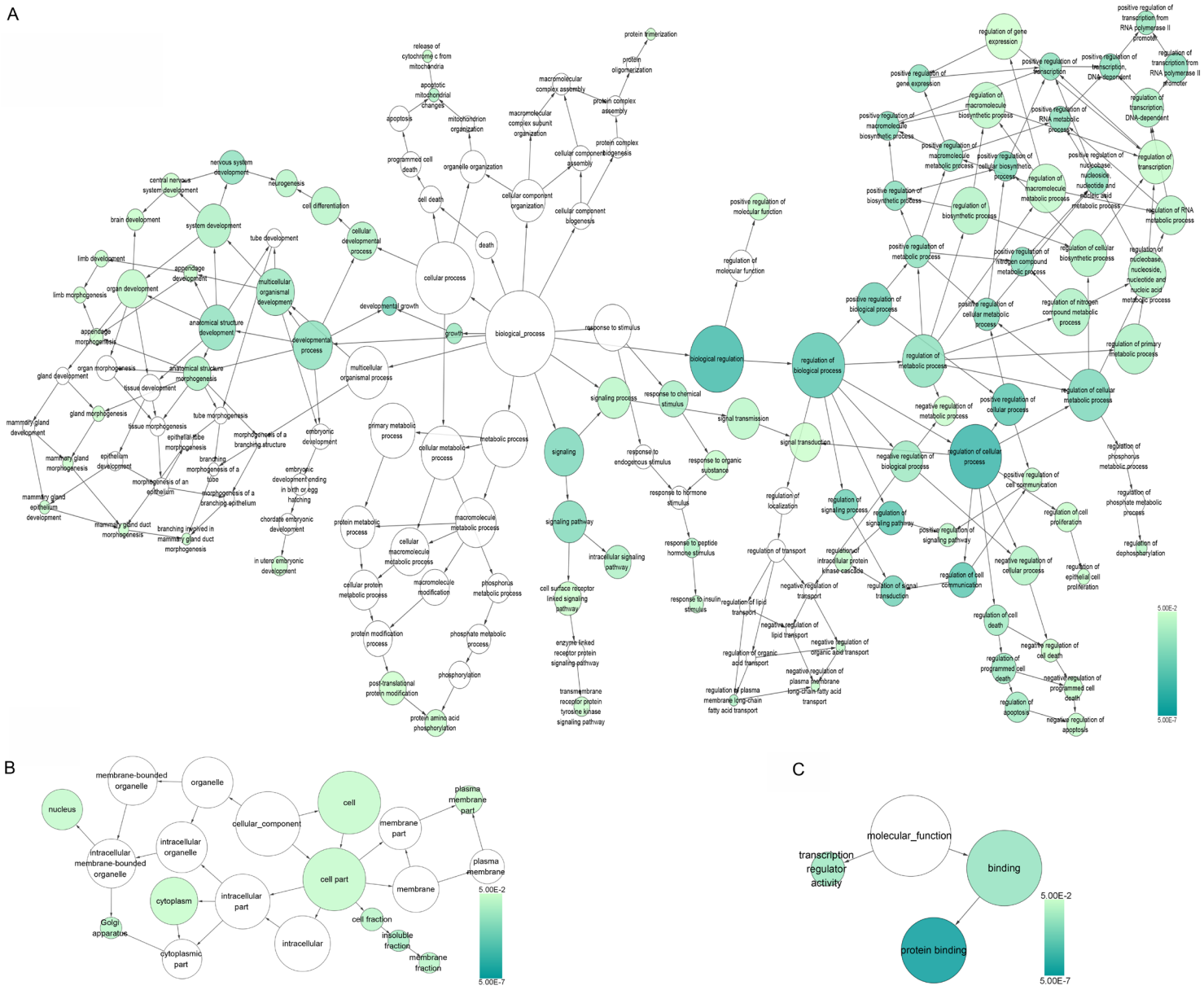

Figure 6. Signaling pathways of putative miR-146b-5p target genes by GO term enrichment. A: Biological process (BP); B: Cellular component (CC); C: Molecular function (MF).

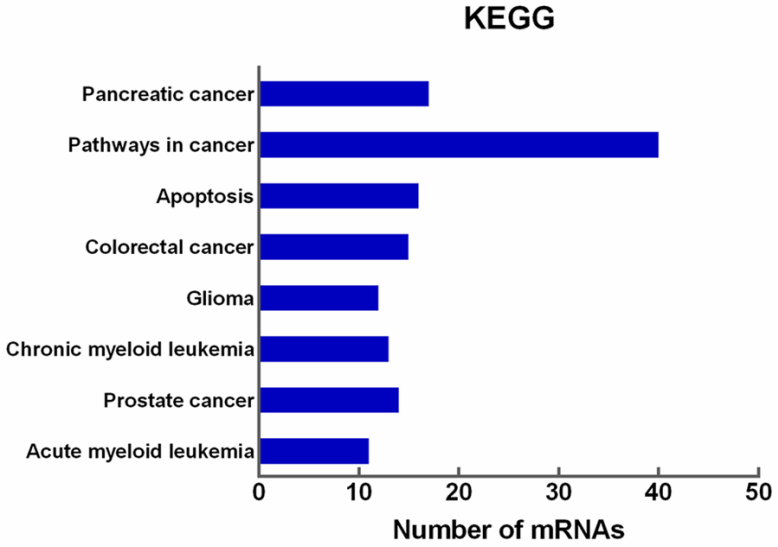

Figure 7. Functional annotation of DAVID KEGG pathways enriched by the putative target mRNAs of miR-146b-5p. The eight most significant signaling pathways are shown.

Optimal candidate targets of miR-146b-5p in PTC

From the GSE76050 dataset, 6273 differentially expressed genes were identified as potential targets with the analysis described in the methods. With respect to the twelve miRNA databases, 4228 genes were identified as predicted targets of miR-146b-5p. Taking the intersection of the two sets of candidates, 994 genes were considered to be optimal candidate targets of miR-146b-5p in PTC.

Functional annotation of target genes

The PPI network consisted of a total of 249 nodes and 180 edges. The following genes with a degree value greater than six were identified as hub genes: CBL (degree=14), CRK (degree=9), FURIN (degree=9), JAK2 (degree=8), FLT3 (degree=8), PLCG1 (degree=8), DOK1 (degree=7), CDK5 (degree=7), CSK (degree=7), and PIA S4 (degree=7).

According to the results of GO analysis, the targets of miR-146b-5p were significantly involved in biological processes including intracellular signaling cascade, regulation of programmed cell death, and positive regulation of cellular biosynthetic processes. Among the cellular components, the targets were most enriched in the insoluble fraction, cell fraction, and membrane fraction. In terms of molecular function, the targets were significantly associated with transcriptional regulator activity and transcriptional activator activity (**Figures 5** and **6**). Moreover, KEGG pathway analysis indicated that the targets of miR-146b-5p were closely associated with 36 signaling pathways, specifically Pancreatic cancer, Pathways in cancer, and Apoptosis (**Figure 7**). These potential targets of miR-146b-5p from the top three KEGG pathways were shown in heatmaps by GSEA (**Figures 8-10**). The PPI maps in **Figure 11** showed the target genes within the two most significant pathways from KEGG analysis. We next further validated the nine genes in the PPI of 'Pathways in cancer', as this is the key pathway associated with all malignancies. Interestingly, two genes, TRAF1 (**Figure 12**) and PML (**Figure 13**), showed down-regulation in their mRNA levels as compared to non-cancerous controls. Consistently, their protein levels were also decreased as shown by The Human Protein Atlas (**Figures 14** and **15**). However, due to the limited number of cases from The Human Protein Atlas, these differences were not statistically significant.

Discussion

MiR-146b-5p has been reported to exert oncogenic or tumor-suppressor effects on the occurrence and progression of various human cancers [30-34]. Overexpression of miR-146b-5p plays an oncogenic role in PTC tissues, and several studies have investigated the molecular function of miR-146-5p and its related target genes in PTC [11, 18, 22-25, 27, 28, 35, 36]. However, little is known about the precise interaction network of miR-146-5p targets. Since a single miRNA can regulate multiple target genes involved in intricate biological processes and signaling pathways, bioinformatics tools including target prediction software, Gene Ontology Enrichment analysis, and Kyoto Encyclopedia of Genes and Genomes pathway analysis may help to achieve a more compre-

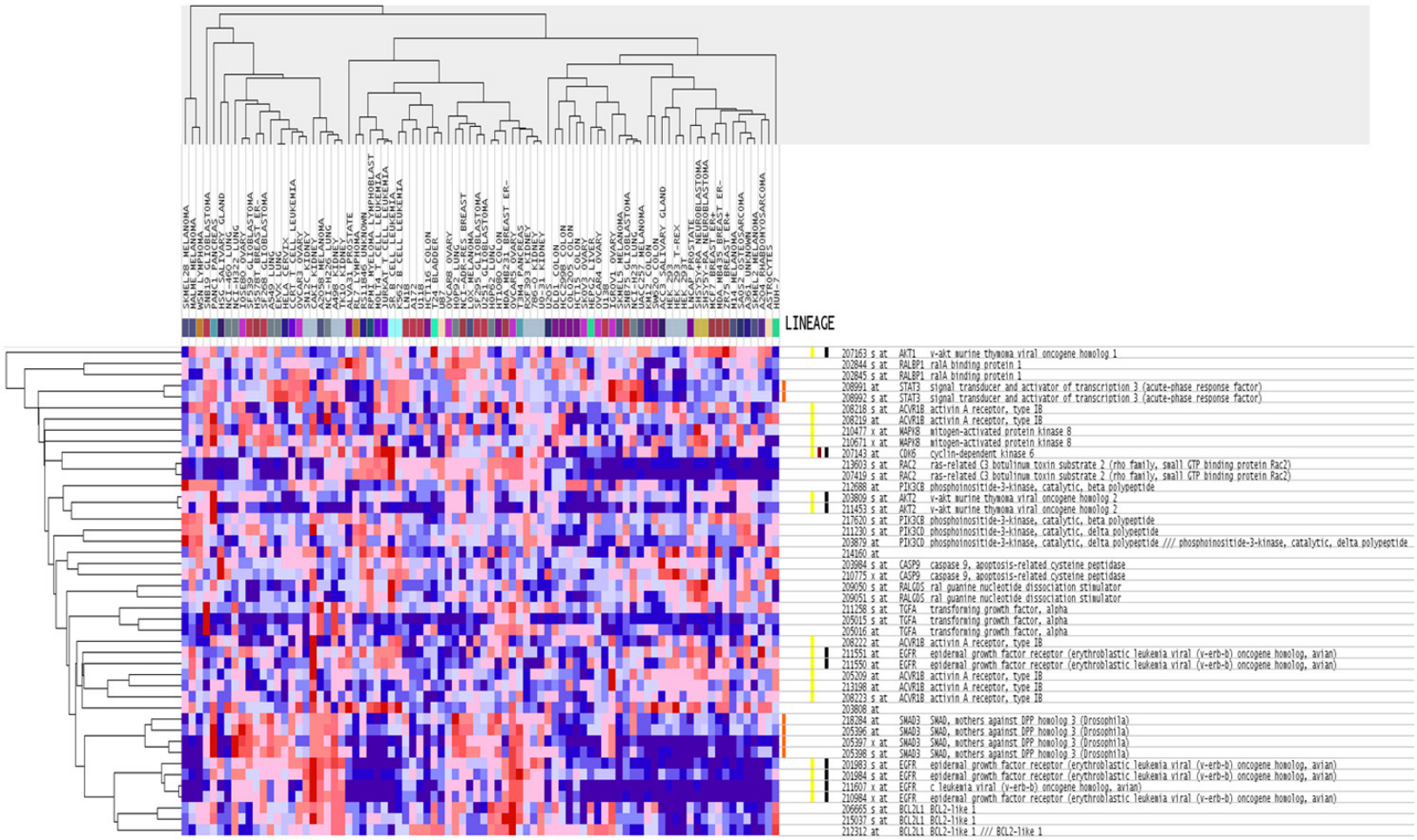

Figure 8. Heatmap of genes from the pathway 'Pancreatic cancer'. The heatmap contains 17 genes and was generated by GSEA (http://software.broadinstitute.org/gsea/datasets.jsp).

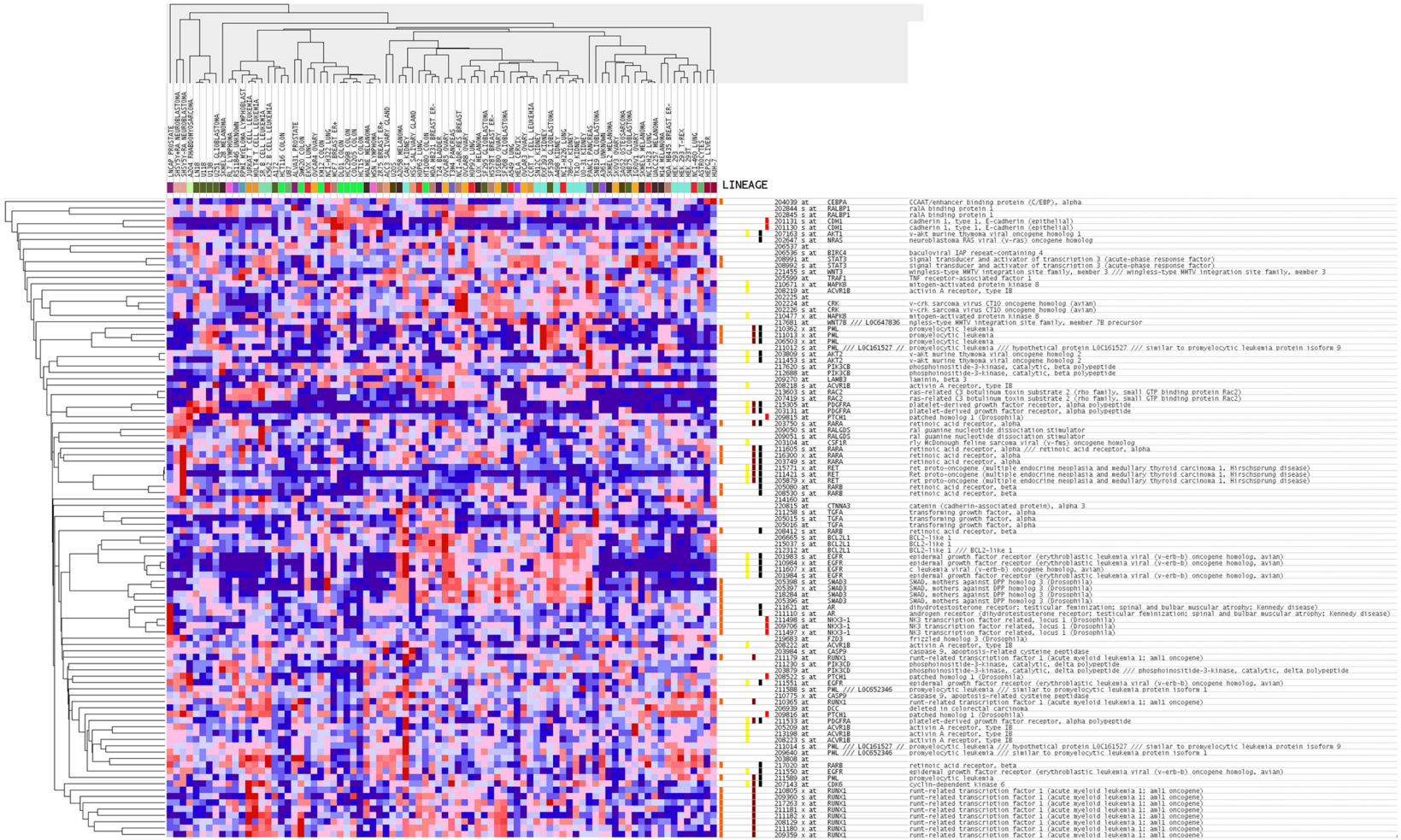

Figure 9. Heatmap of genes from the pathway 'Pathways in cancer'. The heatmap contains 40 genes and was generated by GSEA (http://software.broadinstitute.org/gsea/datasets.jsp).

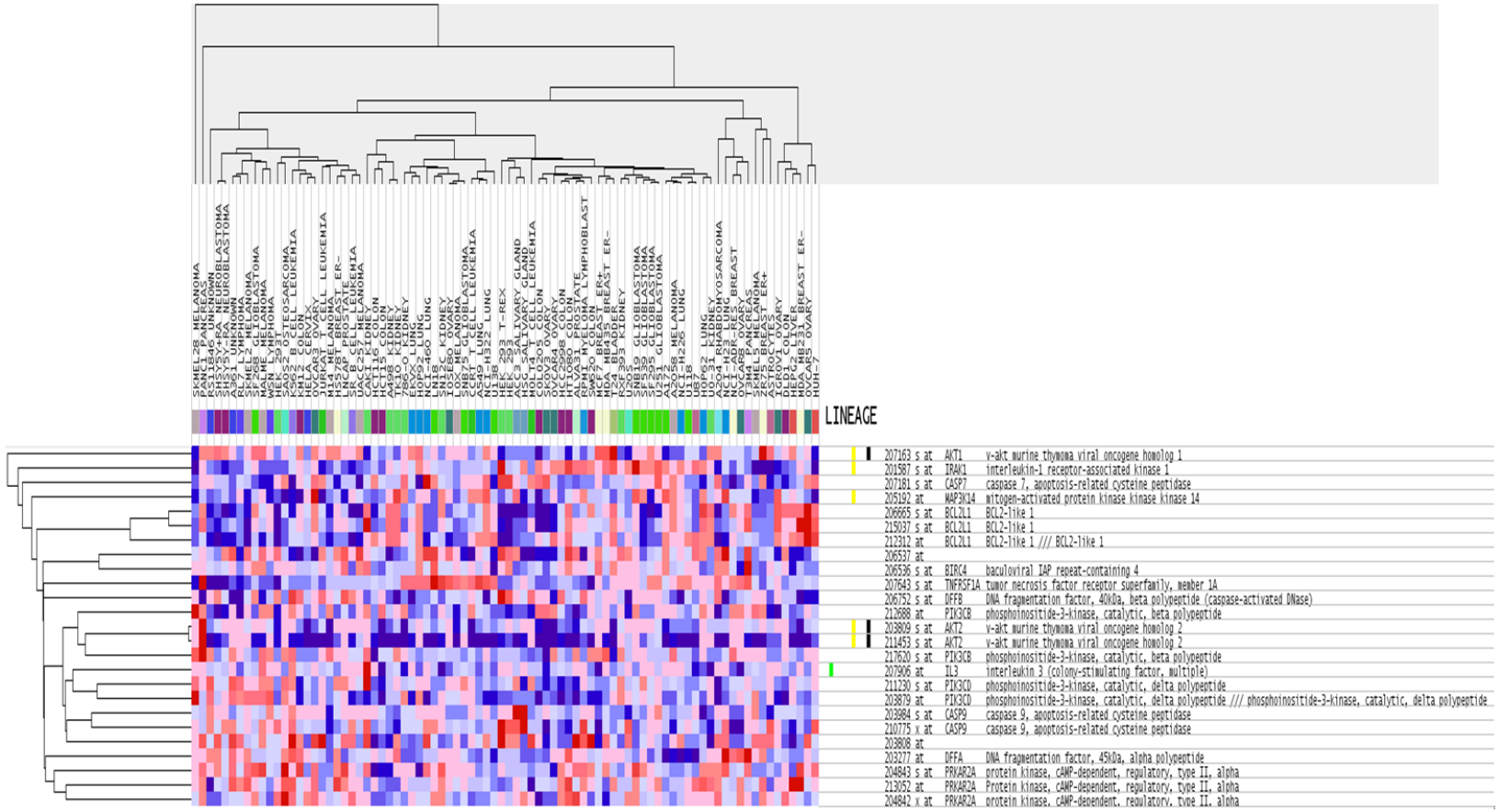

Figure 10. Heatmap of genes from the pathway 'Apoptosis'. The heatmap contains 17 genes and was generated by GSEA (http://software.broadinstitute.org/gsea/datasets.jsp).

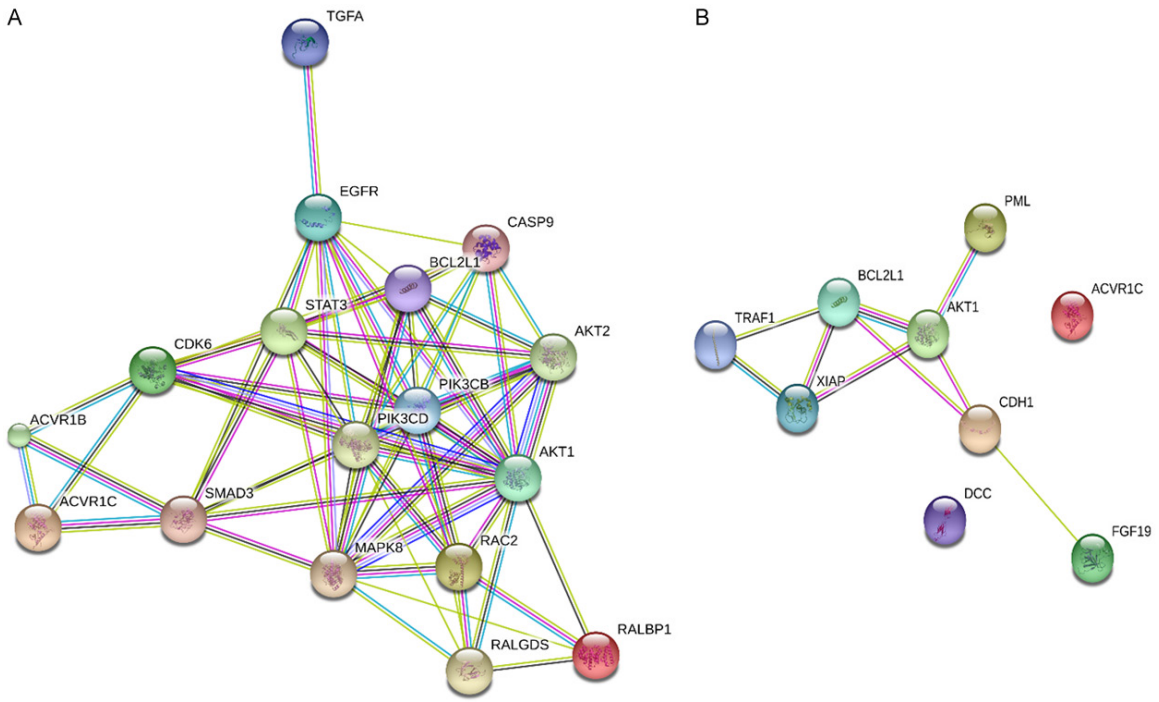

Figure 11. Protein-protein interaction (PPI) network of selected miR-146b-5p target genes. A: Genes from the pathway 'Pancreatic cancer'; B: Genes from the pathway 'Pathways in cancer'.

hensive understanding of the molecular mechanisms behind miR-146b-5p in PTC [37-40].

Our set of 994 probable candidate target genes of miR-146b-5p originated from the intersection of genes found in the GSE76050 dataset comparing miR-146b-5p and mock-transfected cells, with genes identified by the twelve online prediction programs, to increase the probability that these genes were truly target genes of miR-146b-5p in PTC. Among the numerous target genes of miR-146b-5p, hub genes with extensive connections with other target genes might be the most crucial downstream molecules, thus focusing on the hub genes of miR-146b-5p targets will allow us to dive deeper into the underlying mechanism. The hub genes identified from the PPI network revealed potential key targets in the pathogenesis of miR-146b-5p-related PTC. Some of the hub genes, including CBL, CrK, Furin, and CDK5, play pivotal roles in regulating multiple biological processes through signaling transduction or interactions with their corresponding substrates. The CBL family, a class of ubiquitin ligases, might act as tumor suppressors in human cancers by ubiquitinating active RTKs, promoting their subsequent degradation [41]. CrK is a signaling adaptor protein that modulates cell motility, proliferation, and invasion by activating small GTPases including Ras, Rac, and Rap [42]. Furin belongs to the proprotein convertase (PC) family and cleaves proteins vital to the progression and metastasis of cancer cells including IGF1R, VEGF-C, PDGF and MT1-MMP [43]. CDK5 is a member of the cyclin-dependent kinase (CDK) family, which are involved in the regulation of neuronal migration, synaptic activity and neuronal cell survival and death [44-47]. Abnormal expression of these proteins was reported in previous studies to be associated with various human cancers. Furthermore, missense mutations of CBL genes have been discovered in PTC [48, 49], which increases the robustness of our results. The function of these genes described above might help explain the molecular mechanism of miR-146b-5p in PTC. Moreover, some hub genes, such as JAK2, FLT3, DOK1, and PIAS4, play important roles in specific cancers including leukemia and renal clear-cell carcinoma [50-58]. We hypothesize that these genes may exert influences on the progression of PTC through similar interactions as in other cancers, or through other unknown molecular mechanisms.

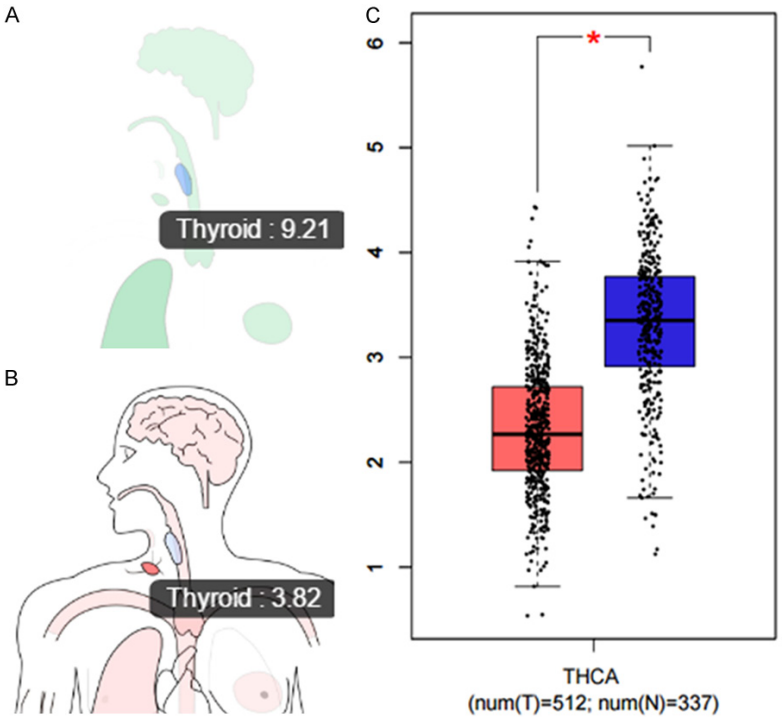

Figure 12. mRNA levels of the hub gene TRAF1 from TCGA data. Median expression of TRAF1 in the normal thyroid gland (A) and tumor samples (B) in bodymap. (C) Gene expression of TRAF1 across all tumor samples (Red) and paired normal tissues (Blue) of thyroid cancer. Bar heights represent the median expression from tumors or normal tissue. (Bar plot, Log2(TPM + 1) Scale). Data were downloaded from GEPIA.

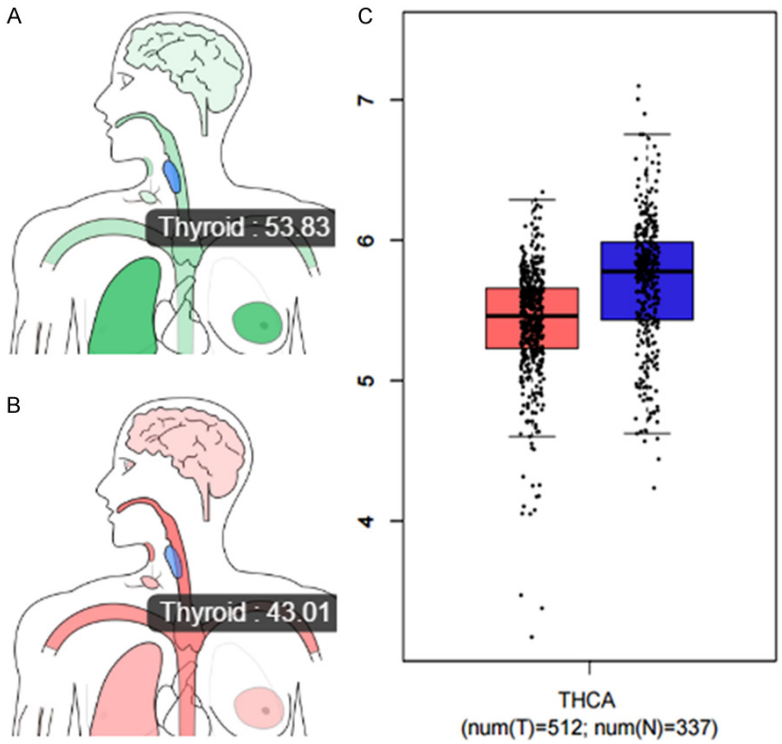

Figure 13. mRNA levels of the hub gene PML from TCGA data. Median expression of PML in the normal thyroid gland (A) and tumor samples (B) in bodymap. (C) Gene expression of PML across all tumor samples (Red) and paired normal tissues (Blue) of thyroid cancer. Bar heights represent the median expression from tumors or normal tissue. (Bar plot, Log2(TPM + 1) Scale). Data were downloaded from GEPIA.

After identifying the hub genes of miR-146b-5p, we further carried out GO enrichment analysis. These results revealed that the target genes of miR-146b-5p were most significantly associated with GO terms related to cell death, apoptosis, and transcriptional activity, which implies that the target genes of miR-146b-5p may influence the malignant behavior of PTC by regulating these biological processes and molecular functions. Signaling pathways are important forms of interaction between molecules. Therefore, analysis of significant signaling pathways is also indispensable for a more thorough understanding of the molecular mechanisms of miR-146b-5p in PTC. According to results from the KEGG pathway analysis, the ten most significant pathways were all closely correlated with cancers. Most of these pathways were directly associated with human cancers, including Pancreatic cancer, Pathways in cancer, Apoptosis, Colorectal cancer, Glioma, Chronic myeloid leukemia, Prostate cancer, and Acute myeloid leukemia. To illustrate the interactions between target genes in these KEGG pathways, three PPI maps corresponding to the three most significant KEGG pathways were constructed. Each of the maps contain nodes with high

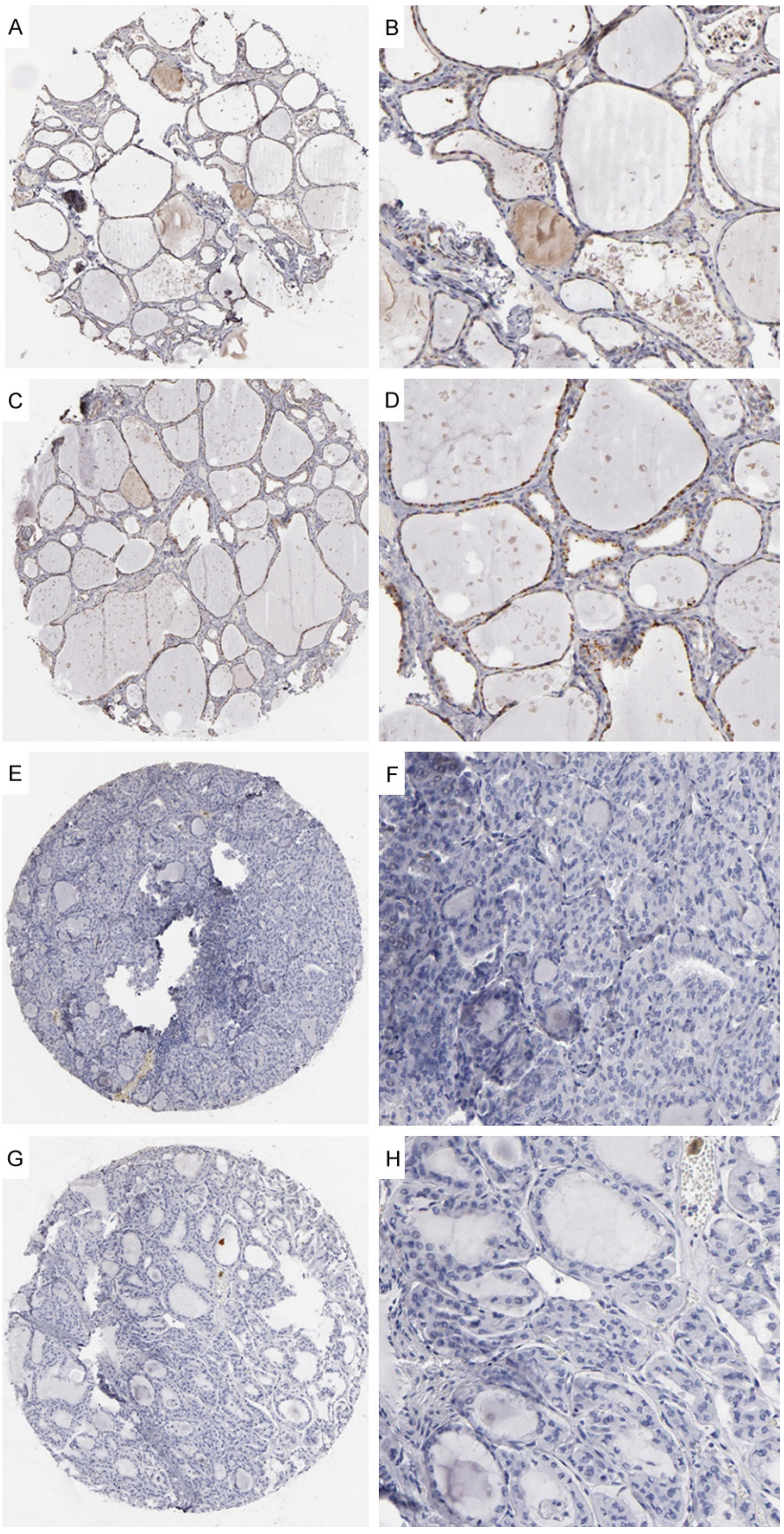

Figure 14. Protein level of the hub gene TRAF1 from The Human Protein Atlas data. TRAF1 protein was detected with the antibody HPA001852, and the staining pattern indicated cytoplasmic/membranous localization. A-D: Thyroid gland (T-96000), Male, age 61, Normal tissue, NOS (M-00100), Patient ID: 2072. Staining: Medium, Intensity: Moderate. E-H: Thyroid gland (T-96000), Male, age 20, Papillary adenocarcinoma, NOS (M-82603), Patient ID: 688. Staining: Not detected, Intensity: Negative. A, C, E, G: x100; B, D, F, H: x400.

degrees (degree≥1), which suggests that these genes may play key roles in their corresponding signaling pathways to contribute to PTC development. It is necessary to highlight two key genes, TRAF1 and PML, which have great potential to be real targets of miR-146b-5p in PTC as shown by the down-regulation of their mRNA and protein levels as assessed by TCGA and The Human Protein Atlas data. This identification of relevant pathways and hub genes may help us to achieve a deeper understanding of the underlying molecular mechanisms of miR-146b-5p in PTC.

In conclusion, miR-146b-5p may play an essential role in PTC by regulating specific target genes and signaling pathways related to cancer, promoting the malignant potential of PTC. Future experimental work is needed to validate these hub genes and signaling pathways.

Acknowledgements

We would like to thank the Funds of Guangxi Health Bureau Research Project (Z2012053), the Scientific Research Project of the Guangxi Education Agency (KY2015YB180), and the Research Project of the Guangxi University of Science and Technology (1419-222). The funders had no role in the study design, data collection and analysis, decision to publish, or preparation of the manuscript. We acknowledge the TCGA, GEPIA, and the Human Protein Atlas for providing the relevant data.

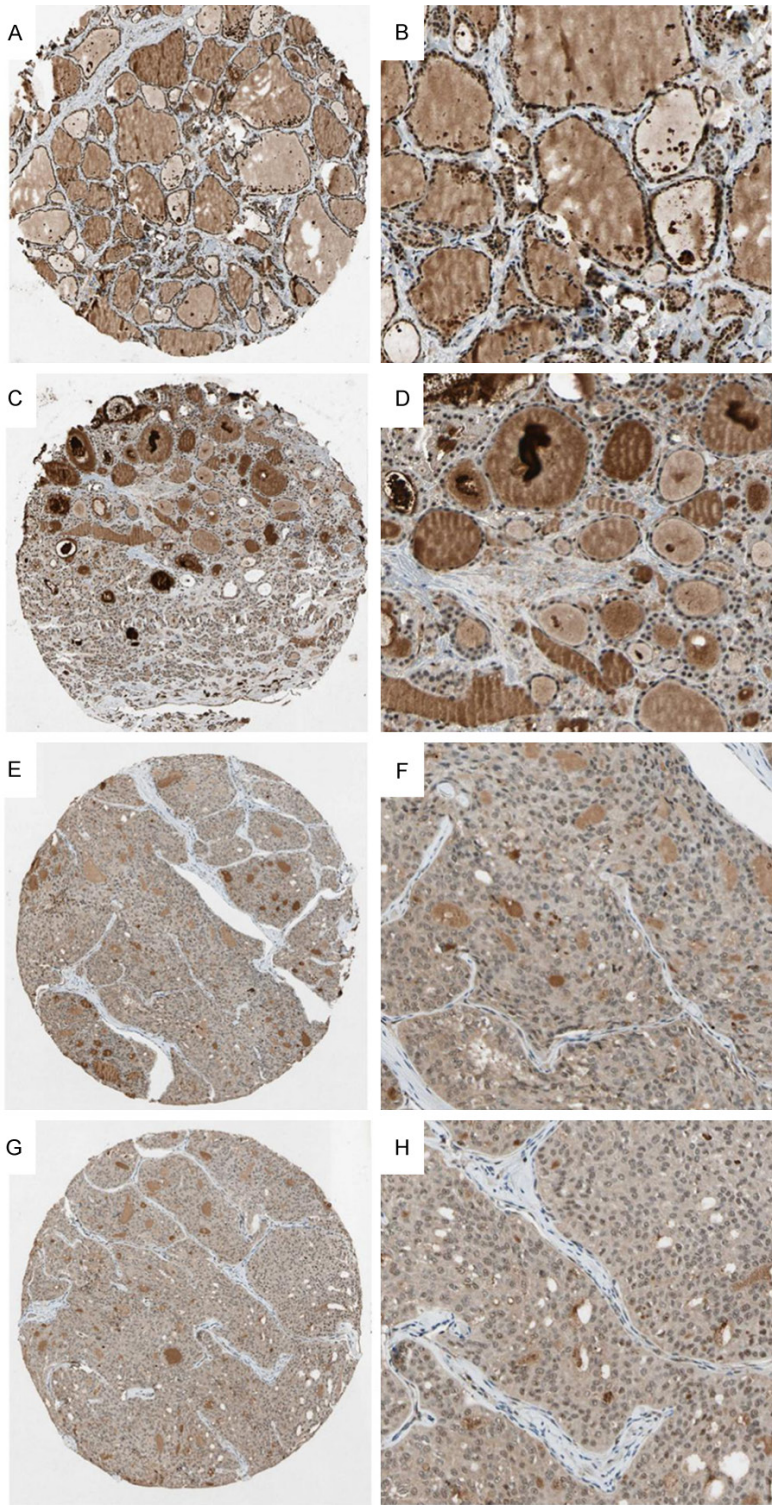

Figure 15. Protein level of the hub gene PML from The Human Protein Atlas data. PML protein was detected with the antibody HPA008312, and the staining pattern indicated cytoplasmic/membranous localization. A-D: Thyroid gland (T-96000), Female, age 44, Normal tissue, NOS (M-00100), Patient ID: 3005. Staining: High, Intensity: Strong. E-H: Thyroid Thyroid gland (T-96000), Male, age 75, Follicular adenoma carcinoma, NOS (M-83303), Patient ID: 3107. Staining: Low, Intensity: Weak. A, C, E, G: x100; B, D, F, H: x400.

Disclosure of conflict of interest

None.

Address correspondence to: Wei Ma, Department of Pathology, The First Affiliated Hospital of Guangxi Medical University, 6 Shuangyong Road, Nanning, Guangxi Zhuang Autonomous Region, People's Republic of China. E-mail: mawei_gxmu@163.com; Hong Yang, Department of Medical Ultrasonography, The First Affiliated Hospital of Guangxi Medical University, 6 Shuangyong Road, Nanning, Guangxi Zhuang Autonomous Region, People's Republic of China. E-mail: yanghonggx@163.com

References

[1] Yin DT, Yu K, Lu RQ, Li X, Xu J and Lei M. Prognostic impact of minimal extrathyroidal extension in papillary thyroid carcinoma. Medicine (Baltimore) 2016; 95: e5794.

[2] Dong S, Meng X, Xue S, Yan Z, Ren P and Liu J. microRNA-141 inhibits thyroid cancer cell growth and metastasis by targeting insulin receptor substrate 2. Am J Transl Res 2016; 8: 1471-1481.

[3] Fagin JA and Wells SA Jr. Biologic and clinical perspectives on thyroid cancer. N Engl J Med 2016; 375: 1054-1067.

[4] Pradhan D, Sharma A and Mohanty SK. Cribriform-morular variant of papillary thyroid carcinoma. Pathol Res Pract 2015; 211: 712-716.

[5] Gambardella C, Tartaglia E, Nunziata A, Izzo G, Siciliano G, Cavallo F, Maurello C, Napolitano S, Thomas G, Testa D, Rossetti G, Sanguinetti A, Avenia N and Conzo G. Clini-

cal significance of prophylactic central compartment neck dissection in the treatment of clinically node-negative papillary thyroid cancer patients. World J Surg Oncol 2016; 14: 247.
[6] Shen J, Wang S, Zhao X, Shao X, Jiang X, Dai Y, Xu S and Pan X. Skull metastasis from follicular thyroid carcinoma: report of three cases and review of literature. Int J Clin Exp Pathol 2015; 8: 15285-15293.
[7] Zhao S, Li L, Wang S, Yu C, Xiao B, Lin L, Cong W, Cheng J, Yang W, Sun W and Cui S. H2O2 treatment or serum deprivation induces autophagy and apoptosis in naked mole-rat skin fibroblasts by inhibiting the PI3K/Akt signaling pathway. Oncotarget 2016; 7: 84839-84850.
[8] Sun W, Lan X, Zhang H, Dong W, Wang Z, He L, Zhang T and Liu S. Risk factors for central lymph node metastasis in CN0 papillary thyroid carcinoma: a systematic review and meta-analysis. PLoS One 2015; 10: e0139021.
[9] Lee YS, Kim Y, Jeon S, Bae JS, Jung SL and Jung CK. Cytologic, clinicopathologic, and molecular features of papillary thyroid carcinoma with prominent hobnail features: 10 case reports and systematic literature review. Int J Clin Exp Pathol 2015; 8: 7988-7997.
[10] Prescott JD and Zeiger MA. The RET oncogene in papillary thyroid carcinoma. Cancer 2015; 121: 2137-2146.
[11] Cong D, He M, Chen S, Liu X, Liu X and Sun H. Expression profiles of pivotal microRNAs and targets in thyroid papillary carcinoma: an analysis of the cancer genome atlas. Onco Targets Ther 2015; 8: 2271-2277.
[12] Penna GC, Vaisman F, Vaisman M, Sobrinho-Simoes M and Soares P. Molecular markers involved in tumorigenesis of thyroid carcinoma: focus on aggressive histotypes. Cytogenet Genome Res 2016; 150: 194-207.
[13] Saiselet M, Pita JM, Augenlicht A, Dom G, Tarabichi M, Fimereli D, Dumont JE, Detours V and Maenhaut C. miRNA expression and function in thyroid carcinomas: a comparative and critical analysis and a model for other cancers. Oncotarget 2016; 7: 52475-52492.
[14] Hua K, Jin J, Zhang H, Zhao B, Wu C, Xu H and Fang L. MicroRNA-7 inhibits proliferation, migration and invasion of thyroid papillary cancer cells via targeting CKS2. Int J Oncol 2016; 49: 1531-1540.
[15] Tang W, Liao Z and Zou Q. Which statistical significance test best detects oncomiRNAs in cancer tissues? An exploratory analysis. Oncotarget 2016; 7: 85613-85623.
[16] Sekhon K, Bucay N, Majid S, Dahiya R and Saini S. MicroRNAs and epithelial-mesenchymal transition in prostate cancer. Oncotarget 2016; 7: 67597-67611.
[17] Micolucci L, Akhtar MM, Olivieri F, Rippo MR and Procopio AD. Diagnostic value of microRNAs in asbestos exposure and malignant mesothelioma: systematic review and qualitative meta-analysis. Oncotarget 2016; 7: 58606-58637.
[18] Titov SE, Ivanov MK, Karpinskaya EV, Tsivlikova EV, Shevchenko SP, Veryaskina YA, Akhmerova LG, Poloz TL, Klimova OA, Gulyaeva LF, Zhimulev IF and Kolesnikov NN. miRNA profiling, detection of BRAF V600E mutation and RET-PTC1 translocation in patients from novosibirsk oblast (Russia) with different types of thyroid tumors. BMC Cancer 2016; 16: 201.
[19] Vitiello M, Valentino T, De Menna M, Crescenzi E, Francesca P, Rea D, Arra C, Fusco A, De Vita G, Cerchia L and Fedele M. PATZ1 is a target of miR-29b that is induced by Ha-Ras oncogene in rat thyroid cells. Sci Rep 2016; 6: 25268.
[20] Li JH, Zhang SQ, Qiu XG, Zhang SJ, Zheng SH and Zhang DH. Long non-coding RNA NEAT1 promotes malignant progression of thyroid carcinoma by regulating miRNA-214. Int J Oncol 2017; 50: 708-716.
[21] Li Z, Huang X, Xu J, Su Q, Zhao J and Ma J. miR-449 overexpression inhibits papillary thyroid carcinoma cell growth by targeting RET kinase-beta-catenin signaling pathway. Int J Oncol 2016; 49: 1629-1637.
[22] Panebianco F, Mazzanti C, Tomei S, Aretini P, Franceschi S, Lessi F, Di Coscio G, Bevilacqua G and Marchetti I. The combination of four molecular markers improves thyroid cancer cytologic diagnosis and patient management. BMC Cancer 2015; 15: 918.
[23] Lima CR, Geraldo MV, Fuziwara CS, Kimura ET and Santos MF. MiRNA-146b-5p upregulates migration and invasion of different Papillary Thyroid Carcinoma cells. BMC Cancer 2016; 16: 108.
[24] Zhang Y, Xu D, Pan J, Yang Z, Chen M, Han J, Zhang S, Sun L and Qiao H. Dynamic monitoring of circulating microRNAs as a predictive biomarker for the diagnosis and recurrence of papillary thyroid carcinoma. Oncol Lett 2017; 13: 4252-4266.
[25] Ma W, Zhao X, Liang L, Wang G, Li Y, Miao X and Zhao Y. miR-146a and miR-146b promote proliferation, migration and invasion of follicular thyroid carcinoma via inhibition of ST8SIA4. Oncotarget 2017; 8: 28028-28041.
[26] Wang S, Chen Y and Bai Y. p21 participates in the regulation of anaplastic thyroid cancer cell proliferation by miR-146b. Oncol Lett 2016; 12: 2018-2022.
[27] Ab Mutalib NS, Othman SN, Mohamad Yusof A, Abdullah Suhaimi SN, Muhammad R and Jamal R. Integrated microRNA, gene expression and transcription factors signature in papillary

thyroid cancer with lymph node metastasis. PeerJ 2016; 4: e2119.
[28] Czajka AA, Wojcicka A, Kubiak A, Kotlarek M, Bakula-Zalewska E, Koperski L, Wiechno W and Jazdzewski K. Family of microRNA-146 regulates RARbeta in Papillary Thyroid Carcinoma. PLoS One 2016; 11: e0151968.
[29] Xu E, Zhao J, Ma J, Wang C, Zhang C, Jiang H, Cheng J, Gao R and Zhou X. miR-146b-5p promotes invasion and metastasis contributing to chemoresistance in osteosarcoma by targeting zinc and ring finger 3. Oncol Rep 2016; 35: 275-283.
[30] Zhu Y, Wu G, Yan W, Zhan H and Sun P. miR-146b-5p regulates cell growth, invasion, and metabolism by targeting PDHB in colorectal cancer. Am J Cancer Res 2017; 7: 1136-1150.
[31] Cinegaglia NC, Andrade SC, Tokar T, Pinheiro M, Severino FE, Oliveira RA, Hasimoto EN, Cataneo DC, Cataneo AJ, Defaveri J, Souza CP, Marques MM, Carvalho RF, Coutinho LL, Gross JL, Rogatto SR, Lam WL, Jurisica I and Reis PP. Integrative transcriptome analysis identifies deregulated microRNA-transcription factor networks in lung adenocarcinoma. Oncotarget 2016; 7: 28920-28934.
[32] Li C, Miao R, Liu S, Wan Y, Zhang S, Deng Y, Bi J, Qu K, Zhang J and Liu C. Down-regulation of miR-146b-5p by long noncoding RNA MALAT1 in hepatocellular carcinoma promotes cancer growth and metastasis. Oncotarget 2017; 8: 28683-28695.
[33] Ding HY, Qian WQ and Xu J. MicroRNA-146b acts as a potential tumor suppressor in human prostate cancer. J BUON 2016; 21: 434-443.
[34] Yang W, Yu H, Shen Y, Liu Y, Yang Z and Sun T. MiR-146b-5p overexpression attenuates stemness and radioresistance of glioma stem cells by targeting HuR/lincRNA-p21/beta-catenin pathway. Oncotarget 2016; 7: 41505-41526.
[35] Chou CK, Liu RT and Kang HY. MicroRNA-146b: a novel biomarker and therapeutic target for human papillary thyroid cancer. Int J Mol Sci 2017; 18.
[36] Deng X, Wu B, Xiao K, Kang J, Xie J, Zhang X and Fan Y. MiR-146b-5p promotes metastasis and induces epithelial-mesenchymal transition in thyroid cancer by targeting ZNRF3. Cell Physiol Biochem 2015; 35: 71-82.
[37] Liu X, Song B, Li S, Wang N and Yang H. Identification and functional analysis of the risk microRNAs associated with cerebral low-grade glioma prognosis. Mol Med Rep 2017; 16: 1173-1179.
[38] Li CY, Xiong DD, Huang CQ, He RQ, Liang HW, Pan DH, Wang HL, Wang YW, Zhu HW and Chen G. Clinical value of miR-101-3p and biological analysis of its prospective targets in breast cancer: a study based on the cancer genome atlas (TCGA) and bioinformatics. Med Sci Monit 2017; 23: 1857-1871.
[39] Fan Q and Liu B. Identification of a RNA-Seq based 8-Long Non-Coding RNA signature predicting survival in esophageal cancer. Med Sci Monit 2016; 22: 5163-5172.
[40] Zhang YH, Chu C, Wang S, Chen L, Lu J, Kong X, Huang T, Li H and Cai YD. The Use of gene ontology term and KEGG pathway enrichment for analysis of drug Half-Life. PLoS One 2016; 11: e0165496.
[41] Lv K, Jiang J, Donaghy R, Riling CR, Cheng Y, Chandra V, Rozenova K, An W, Mohapatra BC, Goetz BT, Pillai V, Han X, Todd EA, Jeschke GR, Langdon WY, Kumar S, Hexner EO, Band H and Tong W. CBL family E3 ubiquitin ligases control JAK2 ubiquitination and stability in hematopoietic stem cells and myeloid malignancies. Genes Dev 2017; 31: 1007-1023.
[42] Dong G, Kalifa R, Nath PR, Gelkop S and Isakov N. TCR crosslinking promotes Crk adaptor protein binding to tyrosine-phosphorylated CD3zeta chain. Biochem Biophys Res Commun 2017; 488: 541-546.
[43] Jaaks P and Bernasconi M. The proprotein convertase furin in tumour progression. Int J Cancer 2017; 141: 654-663.
[44] Pan DH, Zhu ML, Lin XM, Lin XG, He RQ, Ling YX, Su ST, Wickramaarachchi MM, Dang YW, Wei KL and Chen G. Evaluation and clinical significance of cyclin-dependent kinase5 expression in cervical lesions: a clinical research study in Guangxi, China. Eur J Med Res 2016; 21: 28.
[45] Yushan R, Wenjie C, Suning H, Yiwu D, Tengfei Z, Madushi WM, Feifei L, Changwen Z, Xin W, Roodrajeetsing G, Zuyun L and Gang C. Insights into the clinical value of cyclin-dependent kinase 5 in glioma: a retrospective study. World J Surg Oncol 2015; 13: 223.
[46] Wei K, Ye Z, Li Z, Dang Y, Chen X, Huang N, Bao C, Gan T, Yang L and Chen G. An immunohistochemical study of cyclin-dependent kinase 5 (CDK5) expression in non-small cell lung cancer (NSCLC) and small cell lung cancer (SCLC): a possible prognostic biomarker. World J Surg Oncol 2016; 14: 34.
[47] Zhang X, Zhong T, Dang Y, Li Z, Li P and Chen G. Aberrant expression of CDK5 infers poor outcomes for nasopharyngeal carcinoma patients. Int J Clin Exp Pathol 2015; 8: 8066-8074.
[48] Costa V, Esposito R, Ziviello C, Sepe R, Bim LV, Cacciola NA, Decaussin-Petrucci M, Pallante P, Fusco A and Ciccodicola A. New somatic mutations and WNK1-B4GALNT3 gene fusion in papillary thyroid carcinoma. Oncotarget 2015; 6: 11242-11251.
[49] Pitt SC, Hernandez RA, Nehs MA, Gawande AA, Moore FD Jr, Ruan DT and Cho NL. Identifica-

tion of novel oncogenic mutations in thyroid cancer. J Am Coll Surg 2016; 222: 11036-1043, e1032.
[50] Kong X, Sun H, Pan P, Li D, Zhu F, Chang S, Xu L, Li Y and Hou T. How does the L884P mutation confer resistance to Type-II inhibitors of JAK2 kinase: a comprehensive molecular modeling study. Sci Rep 2017; 7: 9088.
[51] Metts J, Bradley HL, Wang Z, Shah NP, Kapur R, Arbiser JL and Bunting KD. Imipramine blue sensitively and selectively targets FLT3-ITD positive acute myeloid leukemia cells. Sci Rep 2017; 7: 4447.
[52] Zhu GZ, Yang YL, Zhang YJ, Liu W, Li MP, Zeng WJ, Zhao XL and Chen XP. High expression of AHSP, EPB42, GYPC and HEMGN predicts favorable prognosis in FLT3-ITD-Negative acute myeloid leukemia. Cell Physiol Biochem 2017; 42: 1973-1984.
[53] Daver N and Kantarjian H. FLT3 inhibition in acute myeloid leukaemia. Lancet Oncol 2017; 18: 988-989.
[54] Zhu S, Zhang C, Weng Q and Ye B. Curcumin protects against acute renal injury by suppressing JAK2/STAT3 pathway in severe acute pancreatitis in rats. Exp Ther Med 2017; 14: 1669-1674.
[55] Kim DH, Park JE, Chae IG, Park G, Lee S and Chun KS. Isoliquiritigenin inhibits the proliferation of human renal carcinoma Caki cells through the ROS-mediated regulation of the Jak2/STAT3 pathway. Oncol Rep 2017; 38: 575-583.
[56] Luo LN, Xie Q, Zhang XG and Jiang R. Osthole decreases renal ischemia-reperfusion injury by suppressing JAK2/STAT3 signaling activation. Exp Ther Med 2016; 12: 2009-2014.
[57] Chu YH, Li H, Tan HS, Koh V, Lai J, Phyo WM, Choudhury Y, Kanesvaran R, Chau NM, Toh CK, Ng QS, Tan PH, Chowbay B and Tan MH. Association of ABCB1 and FLT3 polymorphisms with toxicities and survival in asian patients receiving sunitinib for renal cell carcinoma. PLoS One 2015; 10: e0134102.
[58] Yoon KB, Cho SY, An SJ, Park KR, Lee HJ, Yoon HS, Lee SM, Kim YC and Han SY. Characterization of the aminopyridine derivative KRC-180 as a JAK2 inhibitor. Oncol Lett 2017; 14: 1347-1354.